

# 学位論文

Extracellular N<sup>6</sup>-isopentenyladenosine (i<sup>6</sup>A) addition induces cotranscriptional  
i<sup>6</sup>A incorporation into ribosomal RNAs

(細胞外へのイソペンテニルアデノシン(i<sup>6</sup>A)の添加はリボソームRNAへの転  
写共役的なi<sup>6</sup>Aの取り込みをもたらす)

八木田 麻耶

指導教員

中山 秀樹 教授

熊本大学大学院医学教育部博士課程医学専攻歯科口腔外科学

富澤 一仁 教授

熊本大学大学院医学教育部博士課程医学専攻分子生理学

2022 年度

# 学 位 論 文

論文題名 : Extracellular N<sup>6</sup>-isopentenyladenosine (i<sup>6</sup>A) addition induces cotranscriptional i<sup>6</sup>A incorporation into ribosomal RNAs  
(細胞外へのイソペンテニルアデノシン(i<sup>6</sup>A)の添加はリボソームRNAへの転写共役的なi<sup>6</sup>Aの取り込みをもたらす)

著 者 名 : 八木田 麻耶  
Maya Yakita

指導教員名 : 熊本大学大学院医学教育部博士課程医学専攻歯科口腔外科学 中山 秀樹 教授  
熊本大学大学院医学教育部博士課程医学専攻分子生理学 富澤 一仁 教授

審査委員名 : 臨床病態解析学担当教授 松井 啓隆

呼吸器外科・乳腺外科学担当教授 鈴木 実

耳鼻咽喉科・頭頸部外科学担当教授 折田 頼尚

老化・健康長寿学担当教授 三浦 恭子

2022年度

# Extracellular $N^6$ -isopentenyladenosine ( $i^6A$ ) addition induces cotranscriptional $i^6A$ incorporation into ribosomal RNAs

MAYA YAKITA,<sup>1,2</sup> TAKESHI CHUJO,<sup>1</sup> FAN-YAN WEI,<sup>1,3</sup> MAYUMI HIRAYAMA,<sup>1,2</sup> KOJI KATO,<sup>1</sup> NOZOMU TAKAHASHI,<sup>2</sup> KENTA NAGANUMA,<sup>1</sup> MASASHI NAGATA,<sup>2</sup> KENTA KAWAHARA,<sup>2</sup> HIDEKI NAKAYAMA,<sup>2</sup> and KAZUHITO TOMIZAWA<sup>1</sup>

<sup>1</sup>Department of Molecular Physiology, Faculty of Life Sciences, Kumamoto University, Kumamoto 860-8556, Japan

<sup>2</sup>Department of Oral and Maxillofacial Surgery, Faculty of Life Sciences, Kumamoto University, Kumamoto 860-8556, Japan

<sup>3</sup>Department of Modomics Biology and Medicine, Institute of Development, Aging and Cancer, Tohoku University, Sendai 980-8575, Japan

## ABSTRACT

$N^6$ -isopentenyladenosine ( $i^6A$ ), a modified adenosine monomer, is known to induce cell death upon its addition to the culture medium. However, the molecular fate of extracellularly added  $i^6A$  has yet to be identified. Here we show that  $i^6A$  addition to cell culture medium results in  $i^6A$  incorporation into cellular RNA in several cell lines, including the 5-fluorouracil (5-FU)-resistant human oral squamous cell carcinoma cell line FR2-SAS and its parental 5-FU-sensitive cell line SAS.  $i^6A$  was predominantly incorporated into 18S and 28S rRNAs, and  $i^6A$  incorporation into total RNA was mostly suppressed by treating these cell lines with an RNA polymerase I (Pol I) inhibitor.  $i^6A$  was incorporated into RNA even upon inactivation of TRIT1, the only cellular  $i^6A$ -modifying enzyme. These results indicate that upon cellular uptake of  $i^6A$ , it is anabolized to be used for Pol I transcription. Interestingly, at lower  $i^6A$  concentrations, the cytotoxic effect of  $i^6A$  was substantially more pronounced in FR2-SAS cells than in SAS cells. Moreover, in FR2-SAS cells,  $i^6A$  treatment decreased the rate of cellular protein synthesis and increased intracellular protein aggregation, and these effects were more pronounced than in SAS cells. Our work provides insights into the molecular fate of extracellularly applied  $i^6A$  in the context of intracellular nucleic acid anabolism and suggests investigation of  $i^6A$  as a candidate for a chemotherapy agent against 5-FU-resistant cancer cells.

**Keywords:** RNA modification;  $N^6$ -isopentenyladenosine; 5-fluorouracil; ribosomal RNA; oral squamous cell carcinoma

## INTRODUCTION

Post-transcriptional RNA modifications exist in most RNA species and play pivotal roles in maintaining RNA structural integrity, function, and metabolism (Frye et al. 2016; Agris et al. 2018; Suzuki 2021). To date, more than 150 RNA modifications have been identified in the three domains of life (Boccaletto et al. 2018). RNA modifications are pivotal for life, and aberrations in over 60 human RNA modification enzymes are associated with diseases that frequently manifest as brain dysfunction, mitochondrial diseases, diabetes, or cancer (Wei et al. 2011; Chujo and Tomizawa 2021; Suzuki 2021).

$N^6$ -isopentenyladenosine ( $i^6A$ ) is an RNA modification that exists in tRNAs. The adenosine at tRNA position 37 of specific human tRNA species are post-transcriptionally mod-

ified to  $i^6A$  by tRNA isopentenyltransferase 1 (TRIT1) via recognition of specific anticodon loop sequences (Lamichhane et al. 2011, 2013; Khalique et al. 2020). The *TRIT1* gene has been proposed as a cancer suppressor gene candidate because *TRIT1* expression is low in lung cancer cells and *TRIT1* overexpression suppresses lung cancer cell growth (Spinola et al. 2005). Addition of  $i^6A$  to cell culture media induces cell-cycle-arrest and cell death in cancer cell lines, including colon cancer, bladder cancer, and glioma cell lines (Laezza et al. 2009; Castiglioni et al. 2013; Ciaglia et al. 2017). Also, an increase of endogenous  $i^6A$  monomer level has been shown to exert an antitumor effect by inducing excessive autophagy in a glioma cell line (Yamamoto et al. 2019). Despite these reports on cytotoxicity of  $i^6A$ , the

© 2022 Yakita et al. This article is distributed exclusively by the RNA Society for the first 12 months after the full-issue publication date (see <http://majournal.cshlp.org/site/misc/terms.xhtml>). After 12 months, it is available under a Creative Commons License (Attribution-NonCommercial 4.0 International), as described at <http://creativecommons.org/licenses/by-nc/4.0/>.

Corresponding authors: [tchujo@kumamoto-u.ac.jp](mailto:tchujo@kumamoto-u.ac.jp),

[tomikt@kumamoto-u.ac.jp](mailto:tomikt@kumamoto-u.ac.jp)

Article is online at <http://www.majournal.org/cgi/doi/10.1261/ma.079176.122>.

molecular fate and molecular function of extracellularly added  $i^6A$  monomer has yet to be identified.

At the end of its life, RNA is degraded to nucleoside monomers. In human cells, in comparison to unmodified nucleosides that are salvaged and reused, modified nucleosides are resistant to further degradation and many are exported out of cells through nucleoside transporters called ENT1 and ENT2 (Shi et al. 2021). The modified nucleosides are then circulated in the blood and finally discarded into urine (Mandel et al. 1966; Pane et al. 1992). Recently, a physiological function of a modified nucleoside in the extracellular space has been reported in human and higher mammals. The extracellular  $N^6$ -methyladenosine ( $m^6A$ ) monomer was found to function as a ligand that strongly binds to human A3 adenosine receptor and stimulates intracellular signaling pathways to play physiological roles such as type I allergy (Ogawa et al. 2021).

Various artificial analogs of DNA and RNA nucleosides and nucleobases are used for chemotherapy to cure cancer and viral infection. Generally, these artificial nucleosides and nucleobases inhibit the function of nucleoside biosynthetic enzymes and/or are anabolized where their products are used for nucleotide polymerization by DNA/RNA polymerase (Longley et al. 2003; Eyer et al. 2018). For example, the deoxycytidine analog cytarabine is used in cancer chemotherapy, and adenosine analog remdesivir is used for COVID-19 treatment (Braess et al. 1998; Beigel et al. 2020).

5-fluorouracil (5-FU, Fig. 1A) is a uracil base analog and is commonly used for chemotherapy against various tumors including colon, breast, stomach, and oral cancers (Longley et al. 2003). After 5-FU enters cells, 5-FU is converted to various derivatives including 5-fluorodeoxyuridine monophosphate (5-FdUMP) and 5-fluorouridine triphosphate (5-FUTP). These analogs perturb DNA and RNA synthesis and inhibit specific RNA modification. The fluorine atom at uracil C5-position causes 5-FdUMP to covalently bind to thymidylate synthase to inhibit dTMP synthesis, thereby blocking DNA nucleotide synthesis (Santi et al. 1974). FdUTP can be misincorporated into DNA (Longley et al. 2003) and 5-FUTP used for RNA transcription, whereby it is incorporated into RNA polynucleotides and exists as 5-fluorouridine (5-FUrd, Fig. 1B) within RNA (Longley et al. 2003). Similarly to the case of thymidylate synthase inhibition by 5-FdUMP, 5-fluorouridine taken into tRNAs inhibits the tRNA modification enzymes responsible for 5-methyluridine and pseudouridine by tightly binding to the enzymes, although cytotoxicity by loss of RNA modification may be limited (Spenkuch et al. 2014; Carter et al. 2019). In the human breast cancer cell line MCF-7, 5-FU incorporation into RNA correlated with cytotoxicity, whereas the simultaneous addition of thymidine to bypass the thymidylate synthase block does not cancel this effect. This result suggests that 5-FU incorporation into RNA is the major mechanism of cytotoxic action in MCF-7 cells (Kufe and Major 1981).

5-FU is one of the most effective and commonly used chemotherapeutic agents for various cancers (Longley et al. 2003). However, its clinical applications have been limited by acquired drug resistance of the cancer cells. For example, 5-FU inactivation is initiated by dihydropyridine dehydrogenase (DPYD), an enzyme that incorporates two hydrogen atoms to 5-FU (Lu et al. 1992), and high DPYD expression is observed in some cases of 5-FU-resistant tumors (Salonga et al. 2000). However, despite some advances in the mechanistic understanding of 5-FU resistance, acquired resistance remains a significant limitation to the clinical use of 5-FU. New strategies for overcoming 5-FU-resistant cells are urgently required.

The most common head and neck cancer is oral cancer, especially oral squamous cell carcinoma (OSCC). In the present study, we searched for a means to remove a 5-FU-resistant OSCC cell line and found that  $i^6A$  was able to induce cell death in a 5-FU-resistant OSCC cell line FR2-SAS. Interestingly,  $i^6A$  was substantially more cytotoxic to FR2-SAS cells than the parental 5-FU-sensitive SAS cells. We also revealed that  $i^6A$  addition to the medium induces incorporation of  $i^6A$  into cellular 18S and 28S ribosomal RNAs in an RNA polymerase I transcription-coupled manner. Our work provides insights into the molecular fate of extracellularly added  $i^6A$  and suggests that  $i^6A$  should be considered as a candidate chemotherapy agent for fighting 5-FU-resistant cancer cells.

## RESULTS

### Incorporation of 5-FU into cellular RNA is not decreased in 5-FU-resistant FR2-SAS cells

In search of clues toward eliminating 5-FU resistant cancer cells, we started by comparing our 5-FU-resistant oral squamous cell carcinoma (OSCC) cell line FR2-SAS cells to SAS cells, from which FR2-SAS cells were previously generated (Nagata et al. 2011). In SAS cells, a marked decrease of growth speed was observed when the cells were incubated in the medium containing 15  $\mu$ M 5-FU (Fig. 1C). In contrast, although 5-FU mildly suppressed growth of FR2-SAS cells, the FR2-SAS cells continued to grow even when incubated in the medium containing 15  $\mu$ M 5-FU (Fig. 1C), in accordance with a previous study (Nagata et al. 2011).

Inside cells, 5-FU is converted to 5-fluorouridine (5-FUrd), which is used for RNA transcription (Longley et al. 2003), and 5-FUrd incorporation into RNA correlates with 5-FU cytotoxicity in certain cancer cells (Kufe and Major 1981). Thus, to compare the amount of 5-FUrd intake into RNA of SAS and FR2-SAS cells, the cells were incubated in 5-FU-containing medium and total cellular RNA was degraded to nucleosides for liquid chromatography mass spectrometry (LC-MS) analysis. Upon addition of 5-FU to cell culture medium, total RNA from SAS cells

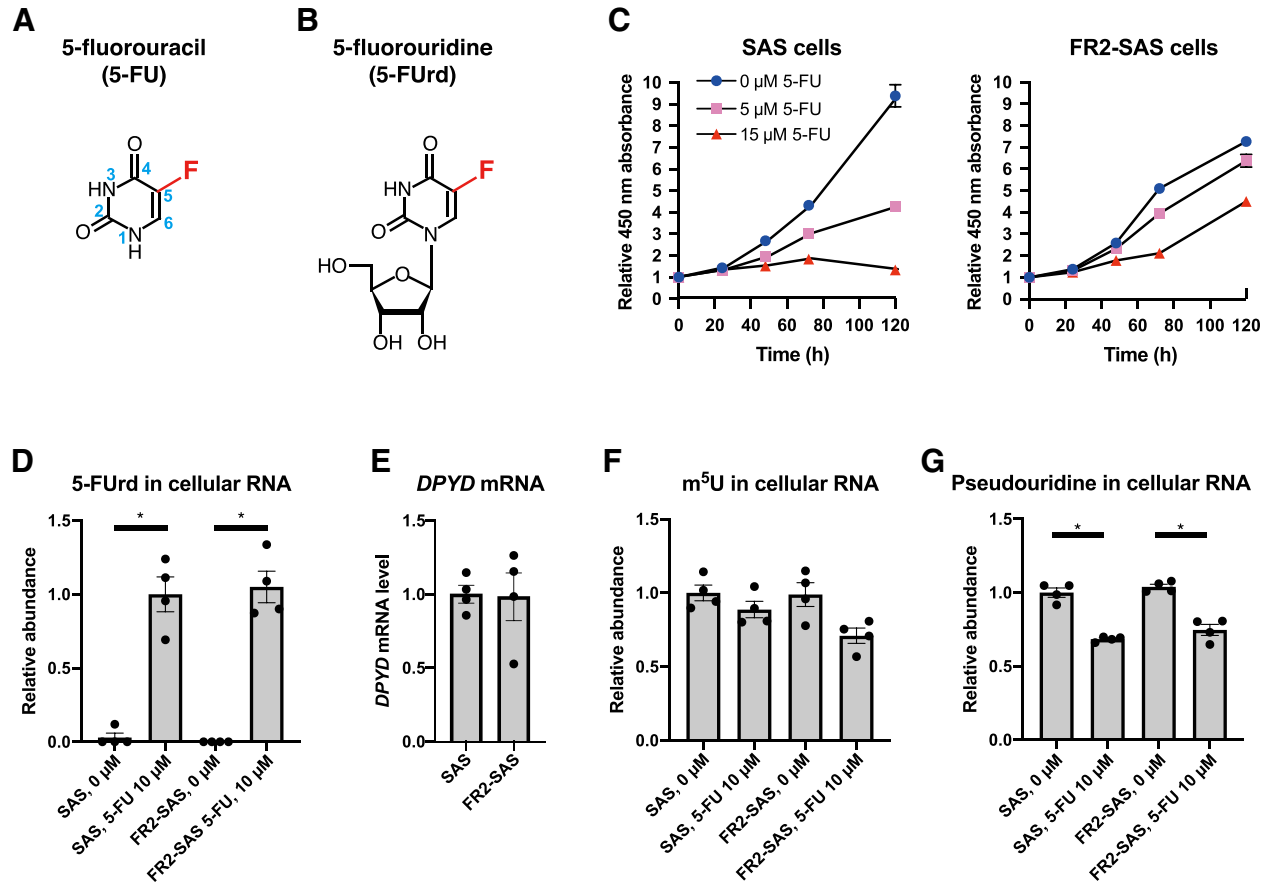


**FIGURE 1.** Incorporation of 5-FU into 5-FU-resistant cell line RNA. (A) Chemical structure of 5-fluorouracil (5-FU). The position numbers are indicated in blue. (B) Chemical structure of 5-fluorouridine (5-FUrd). (C) Cell growth of SAS (left) and FR2-SAS cells (right) cultured in the medium containing 0, 5, or 15 μM 5-FU. Cell growth was quantified by performing WST assay and measuring absorbance at 450 nm. The values are shown as the relative levels versus the mean of 0 h cells. Mean ± standard error of the mean (SEM) from  $n = 8$  biological replicates. (D) 5-FUrd level in cellular RNA from SAS cells and FR2-SAS cells upon addition of 5-FU into cell culture medium. After 48 h of 0 or 10 μM 5-FU addition in the medium, total RNA was collected and digested into nucleosides for LC-MS analysis. Peak areas were normalized by uridine peak areas of the same samples and are shown as the relative levels versus SAS 5-FU 10 μM samples. (E) *DPYD* mRNA levels in SAS cells and FR2-SAS cells. *DPYD* mRNA levels were quantified by RT-qPCR and normalized by *GAPDH* mRNA levels, and are shown as the relative levels versus SAS cells. (F,G) 5-methyluridine (*m*<sup>5</sup>U) and pseudouridine levels in cellular RNA of SAS cells and FR2-SAS cells upon addition of 5-FU into cell culture medium. After 48 h of 0 or 10 μM 5-FU addition in the medium, total RNA was collected and digested into nucleosides for LC-MS analysis. *m*<sup>5</sup>U (F) or pseudouridine (G) peak area was normalized by uridine peak area of the same sample and are shown as the relative levels versus SAS 0 μM samples. Mean ± SEM from  $n = 4$  biological replicates in D–G. (\*)  $P < 0.05$  by Mann–Whitney test.

and FR2-SAS cells showed equivalent 5-FUrd levels (Fig. 1D; Supplemental Fig. 1A), suggesting that 5-FU anabolism into RNA did not substantially differ between 5-FU-resistant FR2-SAS cells and the parental SAS cells. This result was supported by the equivalent *DPYD* mRNA steady-state levels in SAS and FR2-SAS cells (Fig. 1E), the translated protein of which plays a major role in inactivation of 5-FU (Lu et al. 1992).

5-FU is known to suppress tRNA 5-methyluridine (*m*<sup>5</sup>U) modification and pseudouridine modification. Decrease of these modifications may or may not affect cell viability depending on cell lines (Spenkuch et al. 2014; Carter et al. 2019). To investigate the effect of 5-FU on *m*<sup>5</sup>U and pseudouridine modification in SAS and FR2-SAS cells,

we checked the steady-state levels of *m*<sup>5</sup>U and pseudouridine modifications in cellular RNA after 5-FU addition. Upon incubation of cells with 5-FU, while both *m*<sup>5</sup>U and pseudouridine modification levels showed some tendency to decrease in both SAS and FR2-SAS cells, the degrees of changes did not show significant differences between SAS and FR2-SAS cells (Fig. 1F,G; Supplemental Fig. 1B,C). Collectively, these results imply that the 5-FU resistance of OSCC-derived FR2-SAS cells was not acquired through alteration of 5-FU incorporation into cellular RNA or changes in RNA modification levels. Therefore, to induce cell growth arrest or cell death of 5-FU-resistant cells, rather than targeting 5-FU metabolism or transport pathways, a different approach may be more effective.

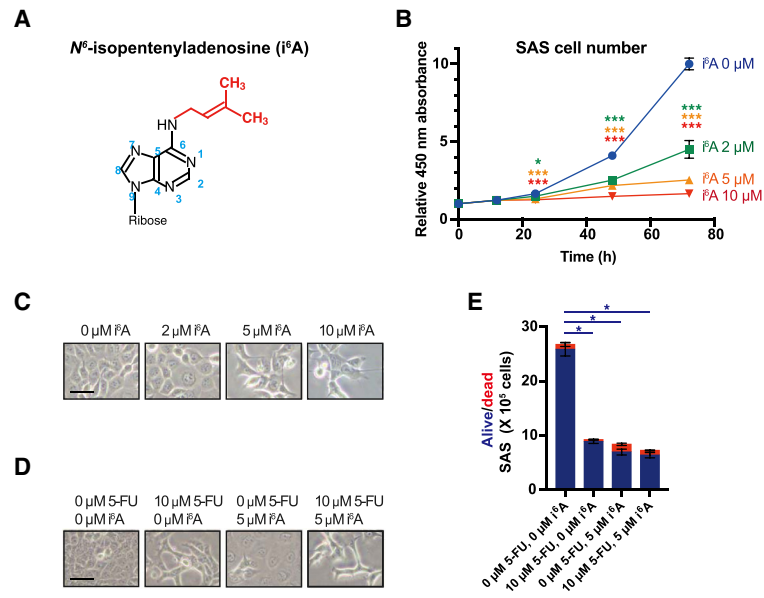
## $i^6A$ suppresses cell growth of SAS cells

Several groups previously showed that  $N^6$ -isopentenyladenosine ( $i^6A$ , Fig. 2A) added to cell culture medium is cytotoxic to various cancer cell lines, such as colon, bladder, and glioma (Laezza et al. 2009; Castiglioni et al. 2013; Ciaglia et al. 2017), prompting us to investigate if  $i^6A$  is cytotoxic to the OSCC cell lines SAS and FR2-SAS. The addition of 2  $\mu M$   $i^6A$  into the cell culture medium decreased SAS cell growth, and addition of 5 or 10  $\mu M$   $i^6A$  further suppressed SAS cell growth (Fig. 2B,C). In SAS cells, using either 5  $\mu M$   $i^6A$  alone, 10  $\mu M$  5-FU alone, or both 5  $\mu M$   $i^6A$  and 10  $\mu M$  5-FU, caused similar levels of cell growth arrest (Fig. 2D,E), showing that the use of  $i^6A$  alone or 5-FU alone is sufficient to exert a similar effect on cell growth suppression in the OSCC cell line SAS.

## Susceptibility of FR2-SAS cells to cell death upon $i^6A$ addition compared to SAS cells

To assess the effects of  $i^6A$  on 5-FU-resistant FR2-SAS cells,  $i^6A$  was added to the cell culture medium of FR2-SAS cells and cell viability monitored (Fig. 3A). Surprisingly, the growth of FR2-SAS was completely stopped by the addition of 2  $\mu M$   $i^6A$  (Fig. 3A). In comparison, SAS cells to which 2  $\mu M$   $i^6A$  was added only partially suppressed cell growth (Fig. 2B). Addition of both 5-FU and  $i^6A$  showed a limited degree of synergistic effect on FR2-SAS cell growth (Fig. 3B,C), showing that use of  $i^6A$  alone is sufficient for cytotoxicity against FR2-SAS cells.

Since FR2-SAS cells were more sensitive to  $i^6A$  than SAS cells, we monitored the effect of  $i^6A$  from smaller concentrations by incubating SAS cells and FR2-SAS cells in medium containing 0, 1, 2, and 4  $\mu M$   $i^6A$ . We then collected nonadherent and adherent cells and distinguished between and counted alive and dead cells using trypan blue staining. SAS cells to which 0, 1, 2, and 4  $\mu M$   $i^6A$  were applied started to die only upon 4  $\mu M$   $i^6A$  addition and only when they were seeded at lower cell density (Fig. 3D, upper and middle panels and Fig. 3E). Conversely, 1  $\mu M$   $i^6A$  significantly decreased FR2-SAS cell number, and 2 or 4  $\mu M$   $i^6A$  caused further cell death in FR2-SAS cells (Fig. 3D, lower panels and Fig. 3F). Even when FR2-SAS cells were cultured at a higher cell density than SAS cells, FR2-SAS cells were more prone to cell death than SAS cells (Fig. 3E, lower graph and



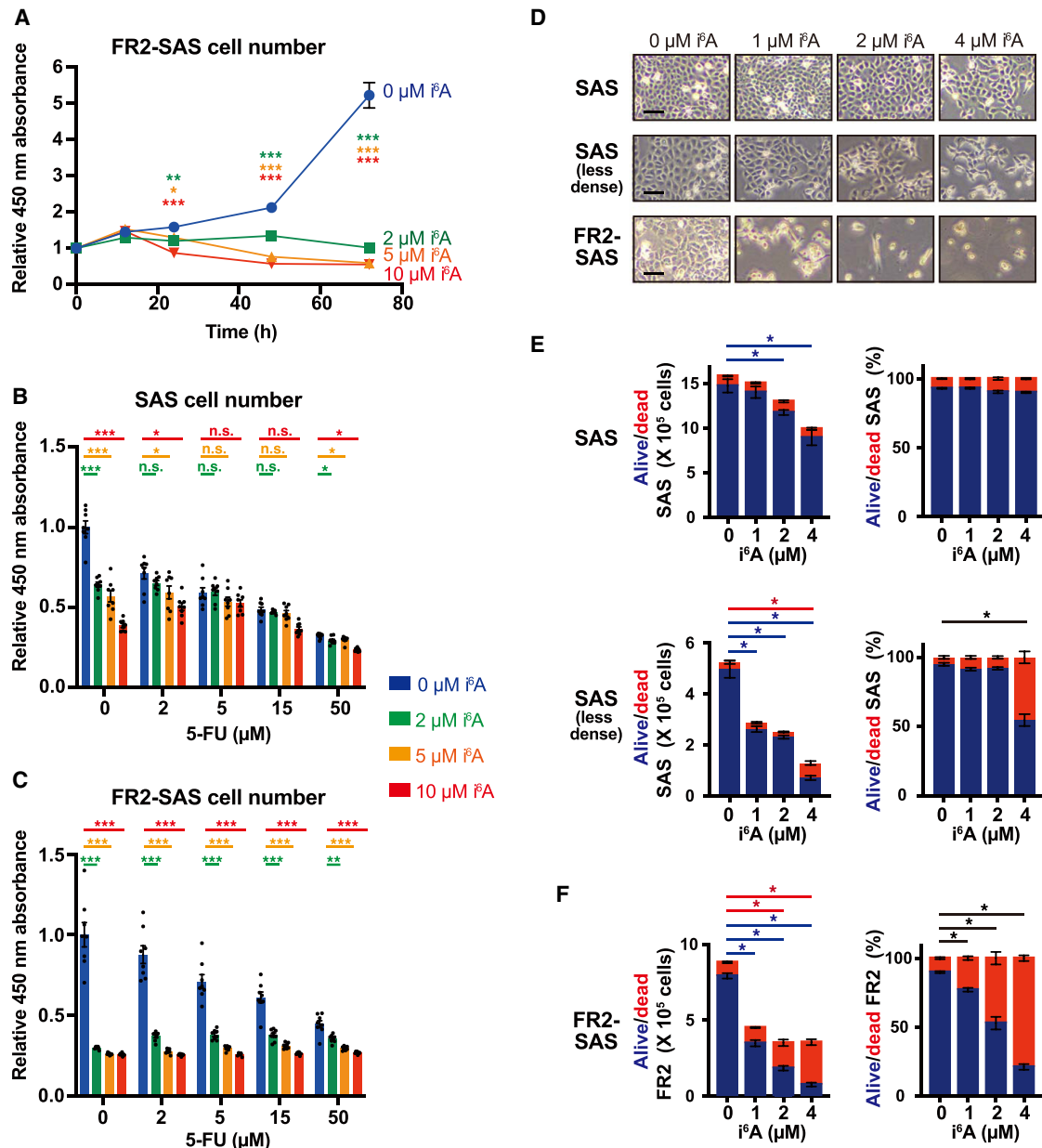
**FIGURE 2.**  $i^6A$ -induced cell growth suppression of oral cancer cell line SAS. (A) Chemical structure of  $N^6$ -isopentenyladenosine ( $i^6A$ ). The position numbers are indicated in blue. (B) Cell growth time course experiment upon addition of 0, 2, 5, or 10  $\mu M$   $i^6A$  in cell culture medium for indicated hours. Cell growth was quantified by performing WST assay and measuring absorbance at 450 nm. The values are shown as the relative levels versus the mean of 0  $\mu M$   $i^6A$  0 h cells. Mean  $\pm$  SEM from  $n = 8$  biological replicates. (C) Microscopic images of SAS cells after 48 h incubation with indicated concentration of  $i^6A$  in the medium. Scale bar, 50  $\mu m$ . (D) Microscopic images of SAS cells after 48 h incubation with indicated concentration of 5-FU and/or  $i^6A$  in the medium. Scale bar, 50  $\mu m$ . (E) Cell numbers of alive (blue) and dead (red) cells after 48 h incubation with indicated concentrations of 5-FU and/or  $i^6A$  in the medium. Alive and dead cells were counted using trypan blue and a cell counting device. Mean  $\pm$  SEM from  $n = 4$  biological replicates. (\*\*\*)  $P < 0.001$ , (\*)  $P < 0.05$  by Mann–Whitney test.

Fig. 3F). Therefore, although FR2-SAS cells are resistant to 5-FU,  $i^6A$  effectively causes cell death in FR2-SAS cells.

## $i^6A$ addition to the medium causes incorporation of $i^6A$ into cellular RNAs

Although  $i^6A$  has been reported to be cytotoxic to several cancer cell lines, the molecular fate and direct molecular function(s) of  $i^6A$  have been unknown. Considering that 5-FU in the medium is taken into the cells, anabolized and incorporated into RNA, we hypothesized that  $i^6A$  in the medium might incorporate into RNA. To investigate this idea, we incubated SAS and FR2-SAS cells in  $i^6A$ -containing medium, collected total cellular RNA, and subjected the samples to RNA digestion and LC-MS analysis. In accordance with our hypothesis, upon  $i^6A$  addition to the medium, the amount of  $i^6A$  contained in the total cellular RNA increased four- to fivefold in both SAS and FR2-SAS cells (“Total RNA” in Fig. 4A; Supplemental Fig. 2).

To investigate whether  $i^6A$  is widely incorporated into various RNA species or specifically incorporated into specific RNA species, we used gel fractionation to collect fractions of tRNA, 18S ribosomal RNA (rRNA), and 28S rRNA.  $N^6$ -threonylcarbamoyladenine ( $t^6A$ ), 2-methylthio- $i^6A$



**FIGURE 3.** *i*<sup>6</sup>A-induced cell death of 5-FU-resistant oral cancer cell line FR2-SAS. (A) Cell growth time course experiment upon addition of 0, 2, 5, or 10  $\mu\text{M}$  *i*<sup>6</sup>A in cell culture medium for indicated number of hours. Cell growth was quantified by performing WST assay and measuring absorbance at 450 nm. The values shown as the relative levels versus the mean of 0  $\mu\text{M}$  *i*<sup>6</sup>A 0 h cells. Mean  $\pm$  SEM from  $n = 8$  biological replicates. (B,C) Cell growth of SAS cells (B) and FR2-SAS cells (C) after 48 h incubation with indicated concentrations of 5-FU and/or *i*<sup>6</sup>A in the medium, quantified by performing WST assay and measuring absorbance at 450 nm, and the values shown as the relative levels versus the mean of 0 h, 0  $\mu\text{M}$  cells. Mean  $\pm$  s.e.m. from  $n = 8$  biological replicates. (D) Microscopic images of SAS cells and FR2-SAS cells after 48 h incubation with indicated concentration of *i*<sup>6</sup>A in the medium. SAS cells were seeded at two densities, that is, at the same density as FR2-SAS cells (top panels) and at lower density (middle panels). Scale bar, 50  $\mu\text{m}$ . (E,F) Cell numbers (left) and percentages (right) of alive (blue) and dead (red) SAS cells (E) and FR2-SAS cells (F) after 48 h incubation with indicated concentrations of *i*<sup>6</sup>A in the medium. SAS cells were seeded at two densities, that is, at the same density as FR2-SAS cells (E, upper graphs) and at lower density (E, lower graphs). Alive and dead cells were counted using trypan blue and a cell counting device. Mean  $\pm$  SEM from  $n = 4$  biological replicates. (\*\*\*)  $P < 0.001$ , (\*\*)  $P < 0.01$ , (\*)  $P < 0.05$  by Mann–Whitney test.

( $\text{ms}^2\text{i}^6\text{A}$ ) and 3-methylcytidine ( $\text{m}^3\text{C}$ ), which are considered to exist exclusively in tRNAs, were enriched in the tRNA fraction and barely detected in rRNA fractions, confirming that the tRNA fractionation was successful (Fig. 4B–D).

Similarly,  $\text{N}^6, \text{N}^6$ -dimethyladenosine ( $\text{m}^6_2\text{A}$ ), which is considered to exist only in 18S rRNA, was enriched in the 18S rRNA fraction, confirming 18S rRNA fractionation was successful (Fig. 4E). In this situation, we unexpectedly

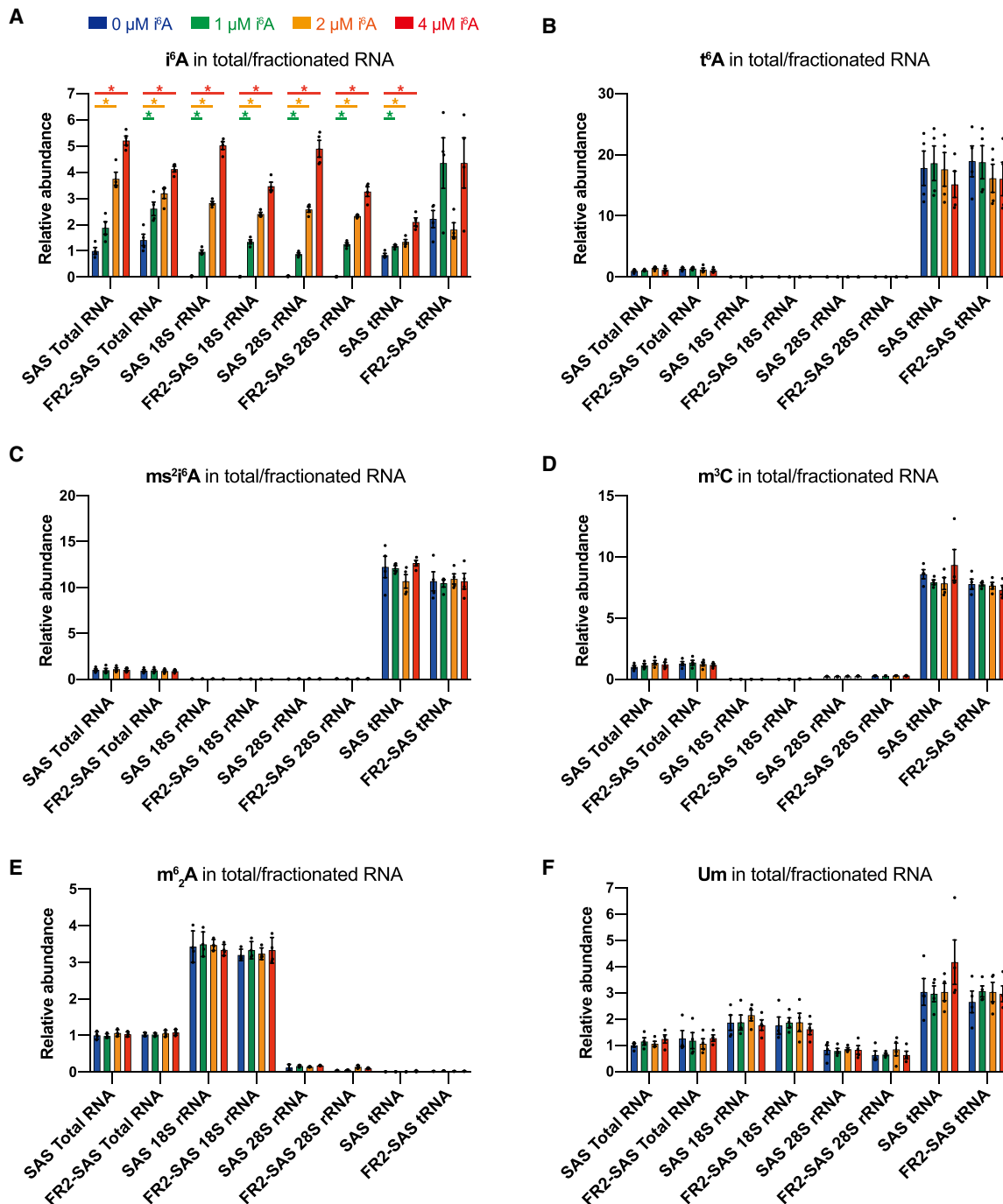


**FIGURE 4.** Incorporation of  $i^6A$  into RNAs upon  $i^6A$  addition to the medium. (A–F) Modified nucleoside levels in RNAs after incubation of SAS or FR2-SAS cells in medium containing no  $i^6A$  (blue), 1  $\mu M$   $i^6A$  (green), 2  $\mu M$   $i^6A$  (yellow), or 4  $\mu M$   $i^6A$  (red) for 24 h. After total RNA extraction, 18S rRNA, 28S rRNA, and tRNA were each fractionated by gel electrophoresis and gel excision, and subjected to digestion to nucleosides and LC-MS analysis.  $i^6A$  (A),  $t^6A$  (B),  $ms^2i^6A$  (C),  $m^3C$  (D),  $m^6_2A$  (E), and Um (F) peak areas were normalized by uridine peak area of the same sample, and the values are shown as the relative levels versus the mean of 0  $\mu M$   $i^6A$  SAS cell total RNA samples. Mean  $\pm$  SEM from  $n = 4$  biological replicates. (\*)  $P < 0.05$  by Mann-Whitney test.

observed substantial increases of  $i^6A$  incorporation into the 18S rRNA and 28S rRNA fractions in both SAS cells and FR2-SAS cells (Fig. 4A; Supplemental Fig. 2). We also attempted to fractionate poly(A)<sup>+</sup> RNA, which is primarily

composed of mRNAs, but could not completely remove contaminations of abundant tRNAs and rRNAs. Thus, poly(A)<sup>+</sup> RNAs could not be analyzed. Considering that rRNAs comprise 80%–90% of cellular RNA, tRNAs

comprise about 10% of cellular RNA, and mRNAs and other noncoding RNAs comprise the remaining few percent, our results indicate that *i*<sup>6</sup>A addition to the cell culture medium predominantly induced *i*<sup>6</sup>A incorporation into 18S and 28S rRNAs.

Apart from the endogenous *i*<sup>6</sup>A at tRNA position 37 incorporated by the TRIT1 enzyme, *i*<sup>6</sup>A addition to the medium slightly increased the *i*<sup>6</sup>A level in the SAS cell tRNA fraction (Fig. 4A). The *i*<sup>6</sup>A level in the FR2-SAS cell tRNA fraction repeatedly fluctuated (Fig. 4A), which may or may not be due to vulnerability of FR2-SAS cells to *i*<sup>6</sup>A. In SAS cell tRNA, if *i*<sup>6</sup>A increase is due to an increased activity of TRIT1-mediated *i*<sup>6</sup>A modification at tRNA position 37, ms<sup>2</sup>*i*<sup>6</sup>A modification in mitochondrial tRNA position 37 might also increase, because *i*<sup>6</sup>A modification within ms<sup>2</sup>*i*<sup>6</sup>A is performed by TRIT1 (Schweizer et al. 2017; Takenouchi et al. 2019). However, upon *i*<sup>6</sup>A addition to the medium, the ms<sup>2</sup>*i*<sup>6</sup>A level did not increase in SAS cells and FR2-SAS cells (Fig. 4C), implying that TRIT1 is irrelevant in this process. In addition, endogenous *i*<sup>6</sup>A at tRNA position 37 is known to promote m<sup>3</sup>C modification at tRNA position 32 in human mitochondria and fission yeast and 2'-O-methyluridine (Um) modification at tRNA position 34 in *E. coli* (Zhou et al. 2015; Arimbasseri et al. 2016; Scholler et al. 2021). However, m<sup>3</sup>C and Um levels did not increase upon *i*<sup>6</sup>A addition to the medium (Fig. 4D,F), further supporting the irrelevancy of TRIT1.

### TRIT1-catalyzed post-transcriptional *i*<sup>6</sup>A modification is not responsible for *i*<sup>6</sup>A incorporation into cellular RNA

Within the cell, the artificial nucleobase analog 5-FU is converted to 5-FUTP and incorporated into RNA, presumably during RNA transcription (Longley et al. 2003). However, to the best of our knowledge, all endogenous RNA modifications are incorporated post-transcriptionally by specific RNA modifying enzymes that act on RNA polynucleotides, with the exception of the inosine monomer, which can be made from the adenosine monomer. We set out to differentiate between whether adding *i*<sup>6</sup>A to the medium induces cotranscriptional or post-transcriptional *i*<sup>6</sup>A incorporation into RNA by RNA-modifying enzymes. We first investigated if inactivation of the only known human endogenous *i*<sup>6</sup>A-modifying enzyme TRIT1 prevents *i*<sup>6</sup>A incorporation upon *i*<sup>6</sup>A addition to the medium. Our rationale was based on observations that various cellular stresses induce recruitment of diverse proteins into the nucleolus (Audas et al. 2012). Thus, TRIT1 could be recruited to the nucleolus upon *i*<sup>6</sup>A-induced cellular stress to promiscuously incorporate *i*<sup>6</sup>A into rRNAs.

To investigate the role of TRIT1 in *i*<sup>6</sup>A incorporation into RNA, we mutated the *TRIT1* gene in HEK293FT cells using the CRISPR/Cas9 system. We obtained *TRIT1* mutant cells that have a 1 nt insertion on one allele and a 14 nt deletion

on the other, each of which causes a frameshift that induces a premature termination codon after translation of several amino acids (Fig. 5A; Supplemental Fig. 3). Using western blot, we confirmed that mature TRIT1 protein was present in the control cell lysate and barely detected in the *TRIT1* mutant cell lysate (Fig. 5B). Because the mutation site and the premature termination codon are near the 3' end of the *TRIT1* open reading frame, a small amount of near-full-length TRIT1 may be synthesized by the pioneer-round translation prior to the nonsense-mediated mRNA decay. However, we confirmed that TRIT1 was dysfunctional in *TRIT1* mutant cells by showing that *i*<sup>6</sup>A contained in the total cellular RNA was reduced to less than one percent compared to the control cells (Fig. 5C).

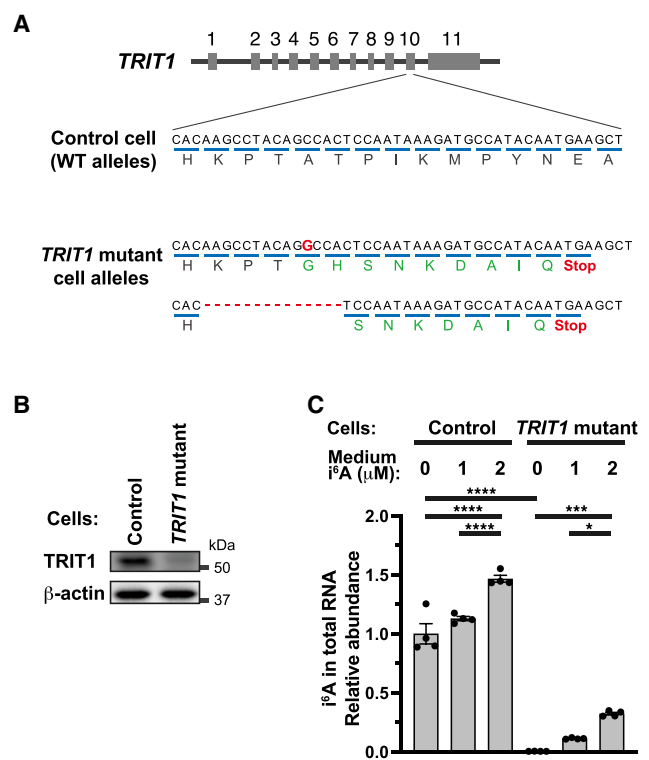


**FIGURE 5.** TRIT1-independent *i*<sup>6</sup>A incorporation into cellular RNA upon *i*<sup>6</sup>A addition to the medium. (A) *TRIT1* alleles in *TRIT1* mutant HEK293FT cells and control HEK293FT cells. Control cells were generated by the same CRISPR/Cas9 cloning procedures using nonhuman DNA targeting guide sequence. Encoded amino acids are indicated under codons. The red G in the mutated allele indicates an extra base insertion. Red lines indicate deletions, and red "Stop" indicates premature termination codon made by frameshift mutations. (B) Western blot of TRIT1 protein in the cells. β-actin is shown as a loading control. (C) *i*<sup>6</sup>A incorporation into control HEK293FT cells or *TRIT1* mutant HEK293FT cells. Cells were incubated in medium containing 0, 1 or 2 μM *i*<sup>6</sup>A for 24 h, and total RNA was extracted and digested to nucleosides for LC-MS analysis. *i*<sup>6</sup>A peak area was normalized by uridine peak area of the same sample, and the values are shown as the relative levels versus the mean of 0 μM *i*<sup>6</sup>A control cell samples. Mean ± SEM from *n* = 4 biological replicates. (\*\*\*\*) *P* < 0.0001, (\*\*\*) *P* < 0.001, (\*\*) *P* < 0.05 by two-way ANOVA followed by Tukey's multiple comparison test.

We then performed LC-MS on total cellular RNA nucleosides and showed that  $i^6A$  addition to the medium induced  $i^6A$  incorporation into total cellular RNA for both control cells and *TRIT1* mutant cells (Fig. 5C). Therefore, *TRIT1*, which is responsible for post-transcriptional  $i^6A$  incorporation at tRNA position 37, does not mediate incorporation of  $i^6A$  into RNA upon  $i^6A$  addition to the medium. Notably,  $i^6A$  addition to the medium caused  $i^6A$  incorporation into RNA not only in SAS and FR2-SAS cells (Fig. 4A), but also in HEK293FT cells (Fig. 5C), suggesting that  $i^6A$  incorporation into cellular RNA upon  $i^6A$  addition to the medium could be a general phenomenon in different types of human cells.

### $i^6A$ incorporation into rRNAs is coupled with Pol I transcription

We next investigated the extent to which RNA polymerase I (Pol I)-dependent rRNA transcription is involved in incorporation of  $i^6A$ , available from the growth medium, into rRNA. For these experiments, we used CX-5461, a potent inhibitor of Pol I (Drygin et al. 2011; Harold et al. 2021). Pol I transcribes 18S, 5.8S and 28S rRNAs in a single precursor RNA containing spacer sequences around the rRNAs. Subsequently, the RNA precursor is processed by specific ribonucleases to produce mature 18S, 5.8S, and 28S rRNAs (Fig. 6A; Aubert et al. 2018). In the Pol I inhibition experiments, we monitored Pol I transcriptional inhibition by detecting the ribosomal RNA precursors using RT-qPCR with primers designed across the spacer RNA and rRNA (Fig. 6A). Upon incubation of SAS or FR2-SAS cells in the cell culture medium containing Pol I inhibitor for 24 h, we detected a reduction of 18S and 28S rRNA precursors (Fig. 6B, blue bars of "Pre-18S" and "Pre-28S") at a comparable level with the previous study (Drygin et al. 2011). We also performed RT-qPCR using primers designed within 18S or 28S rRNA regions. 18S and 28S rRNA steady-state levels, normalized by Pol II-transcribed *GAPDH* mRNA, showed a tendency to decrease to about 75% after 24 h of Pol I inhibitor treatment (Fig. 6B, blue bars of "18S" and "28S"). These decreases also imply that Pol I transcription was largely inhibited. About 75% of 18S and 28S rRNAs remained after 24 h of Pol I inhibitor treatment, presumably due to the long half-lives of cytoplasmic rRNAs.

$i^6A$  addition to the medium resulted in  $i^6A$  incorporation into total RNA of SAS and FR2-SAS cells; however, this was inhibited by the further addition of CX-5461 (Fig. 6C). Some increase of  $i^6A$  levels in total RNA upon only Pol I inhibitor treatment (blue bars in Fig. 6C) might be due to the relative increase of naturally  $i^6A$ -containing tRNA due to a decrease of rRNAs.

Moreover, we showed by the fractionating of 18S and 28S rRNAs isolated by gel excision that  $i^6A$  incorporation into 18S and 28S rRNAs upon  $i^6A$  addition to the medium was inhibited by the further addition of CX-5461 (Fig. 6C).

Collectively, these data show that  $i^6A$  incorporation into 18S and 28S rRNAs did not occur after Pol I transcription, and that  $i^6A$  incorporation into 18S and 28S rRNAs is coupled with Pol I transcription of ribosomal RNAs.

### $i^6A$ induces decrease of cellular protein synthesis and increase of protein aggregation at stronger magnitudes in FR2-SAS cells than in SAS cells

Because  $i^6A$  has a bulky isopentenyl residue (Fig. 2A), incorporation of  $i^6A$  into 18S and 28S rRNAs may alter the 40S and 60S ribosome subunit structure. The ribosome is a ribozyme for protein synthesis (Cech 2000). Thus, ribosomal structural alterations might interfere with protein synthesis, leading to (1) decreased translation rate, and/or (2) decreased translational fidelity, inducing misincorporation of amino acids and misfolding of proteins.

To investigate whether  $i^6A$  incorporation leads to a decreased translation rate, we observed nascent protein synthesis after adding  $^{35}S$ -labeled methionine to the cell culture medium for 35 min, followed by total protein electrophoresis and radio imaging (Fig. 7A). Considering that SAS cells and FR2-SAS cells showed similar levels of  $i^6A$  incorporation into rRNAs (Figs. 4, 6), we initially expected that SAS cells and FR2-SAS cells would show a similar trend. In SAS cells, incubating the cells in the medium containing 0 to 4  $\mu M$   $i^6A$  for 24 h did not change the detectable nascent protein level (Fig. 7A,B). In contrast, to our surprise, in FR2-SAS cells, increasing the medium  $i^6A$  concentration from 0 to 4  $\mu M$  reduced the global protein synthesis rate in a  $i^6A$  dose-dependent manner (Fig. 7A,B).

Next, to determine whether  $i^6A$  incorporation compromises protein quality, we monitored endoplasmic reticulum (ER) stress markers. The extremely high concentration of proteins within the ER makes this organelle susceptible to protein misfolding and aggregation. Accumulation of misfolded or aggregated proteins causes ER stress, which can induce cell death (Hetz et al. 2011). ER stress can be monitored by up-regulation of *BIP*, *CHOP* and *XBP1* mRNAs, as well as by splicing of *XBP1* mRNA (Hetz et al. 2011; Fakruddin et al. 2018). Thus, we determined levels of mRNA for these ER stress markers in SAS cells and FR2-SAS cells after incubation in the medium containing 0, 2, or 4  $\mu M$  of  $i^6A$  for 24 h (Fig. 7C). In SAS cells, ER stress marker mRNA levels were not up-regulated by 2 or 4  $\mu M$   $i^6A$  addition. In contrast, in FR2-SAS cells, we observed clear up-regulations of ER stress marker mRNAs upon 2 or 4  $\mu M$   $i^6A$  addition, suggesting that  $i^6A$ -mediated impaired ER protein quality.

Decreased translational fidelity can increase protein misfolding and aggregation. Thus, to investigate if  $i^6A$  treatment compromises protein quality in FR2-SAS cells by a different method, we monitored protein aggregation using the ProteoStat assay, with  $i^6A$  addition to the medium for 24 h. Although we observed some increase in protein

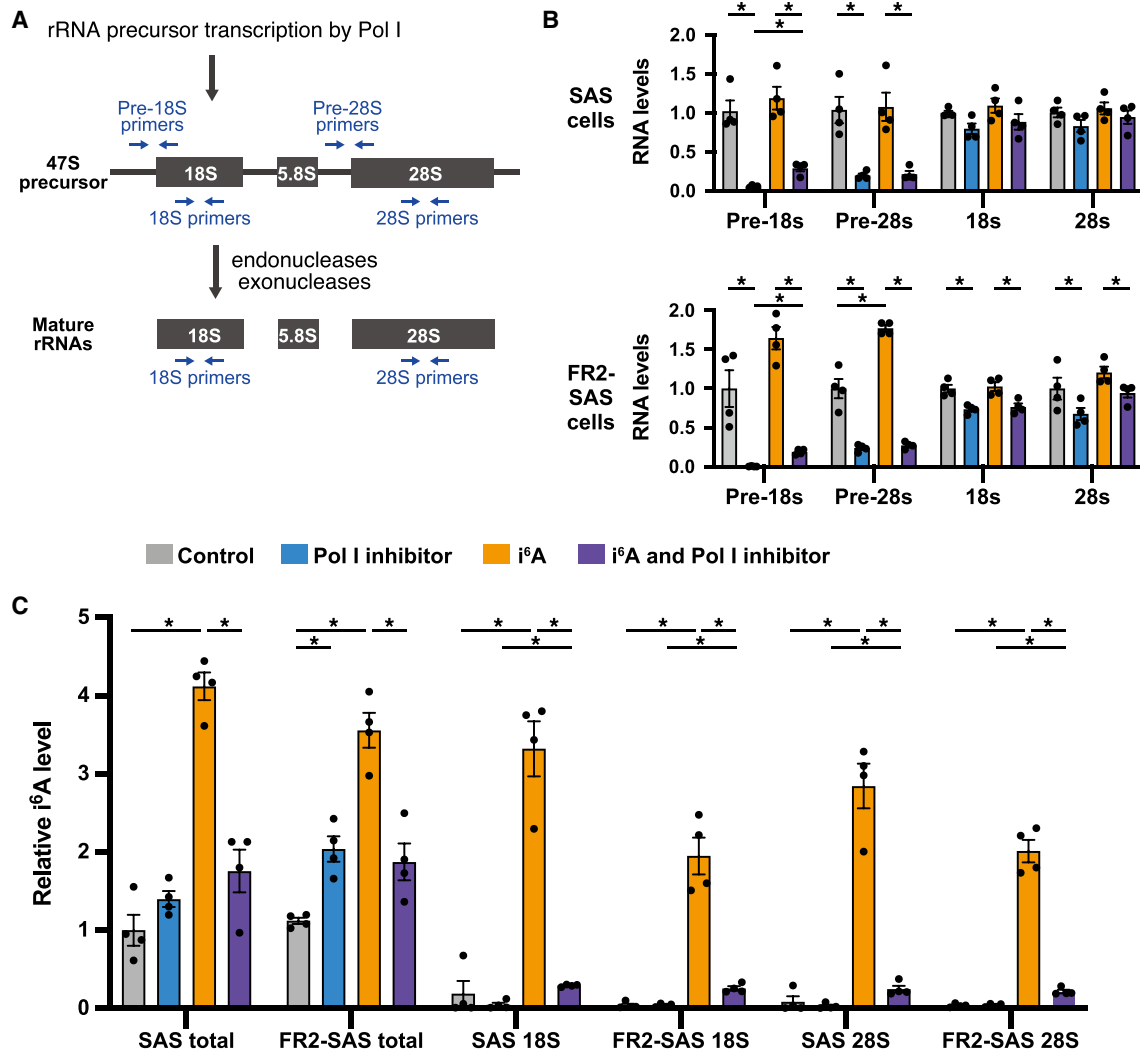


**FIGURE 6.** Pol I transcription-coupled *i*<sup>6</sup>A incorporation into ribosomal RNAs. (A) Schematic of rRNA transcription, processing, and RT-qPCR primers. 18S, 5.8S, and 28S rRNAs are transcribed by Pol I as a polycistronic 47S precursor RNA followed by processing by specific ribonucleases. Pre-18S rRNA primers and pre-28S primers are designed across the boundary of 18S or 28S rRNAs and their adjacent spacer RNAs. (B) RT-qPCR of 18S and 28S rRNAs and their precursors upon addition of 2  $\mu$ M *i*<sup>6</sup>A and/or 2  $\mu$ M Pol I inhibitor, CX-5461 into the medium for 24 h. RNA levels were normalized by Pol II-transcribed *GAPDH* mRNA levels. (C) *i*<sup>6</sup>A level in total cellular RNA, 18S rRNA and 28S rRNA in SAS cells or FR2-SAS cells upon addition of 2  $\mu$ M *i*<sup>6</sup>A and/or 2  $\mu$ M RNA polymerase I inhibitor, CX-5461 into medium for 24 h. Total RNA samples were used to fractionate 18S and 28S rRNAs using agarose gel electrophoresis and gel excision. The RNA samples were digested to nucleosides and subjected to LC-MS analysis. *i*<sup>6</sup>A peak area was normalized by uridine peak area of the same sample. Mean  $\pm$  SEM from  $n = 4$  samples of which RNA samples were independently collected on different days and measured with LC-MS on the same day. (\*)  $P < 0.05$  by Mann-Whitney test.

aggregation in SAS cells, protein aggregation was much more prominent in FR2-SAS cells (Fig. 7D). Collectively, the results shown in Figure 7C and D strongly suggest that *i*<sup>6</sup>A induces more pronounced levels of protein aggregation in FR2-SAS cells than in SAS cells.

## DISCUSSION

5-fluorouracil (5-FU) is commonly used for cancer therapy. However, its clinical applications have often been hampered by acquired drug resistance of cancer cells. Our study revealed that use of another nucleic acid analog,

*i*<sup>6</sup>A, effectively induced cell death of a 5-FU-resistant cell line, FR2-SAS, whereas the parental oral squamous cell carcinoma cell line SAS showed only a mild reduction in cell growth at the same *i*<sup>6</sup>A concentrations. Future studies are needed to investigate whether this effect of *i*<sup>6</sup>A is generalizable to cancer cells resistant to 5-FU and other cancer chemotherapeutic drugs. Also, since artificial nucleoside analogs are used to treat RNA virus infections (Eyer et al. 2018), it may be of importance to test if *i*<sup>6</sup>A is effective against RNA viruses including SARS-CoV-2.

We also discovered that upon *i*<sup>6</sup>A addition to cell growth media, *i*<sup>6</sup>A is incorporated into cellular RNA, especially

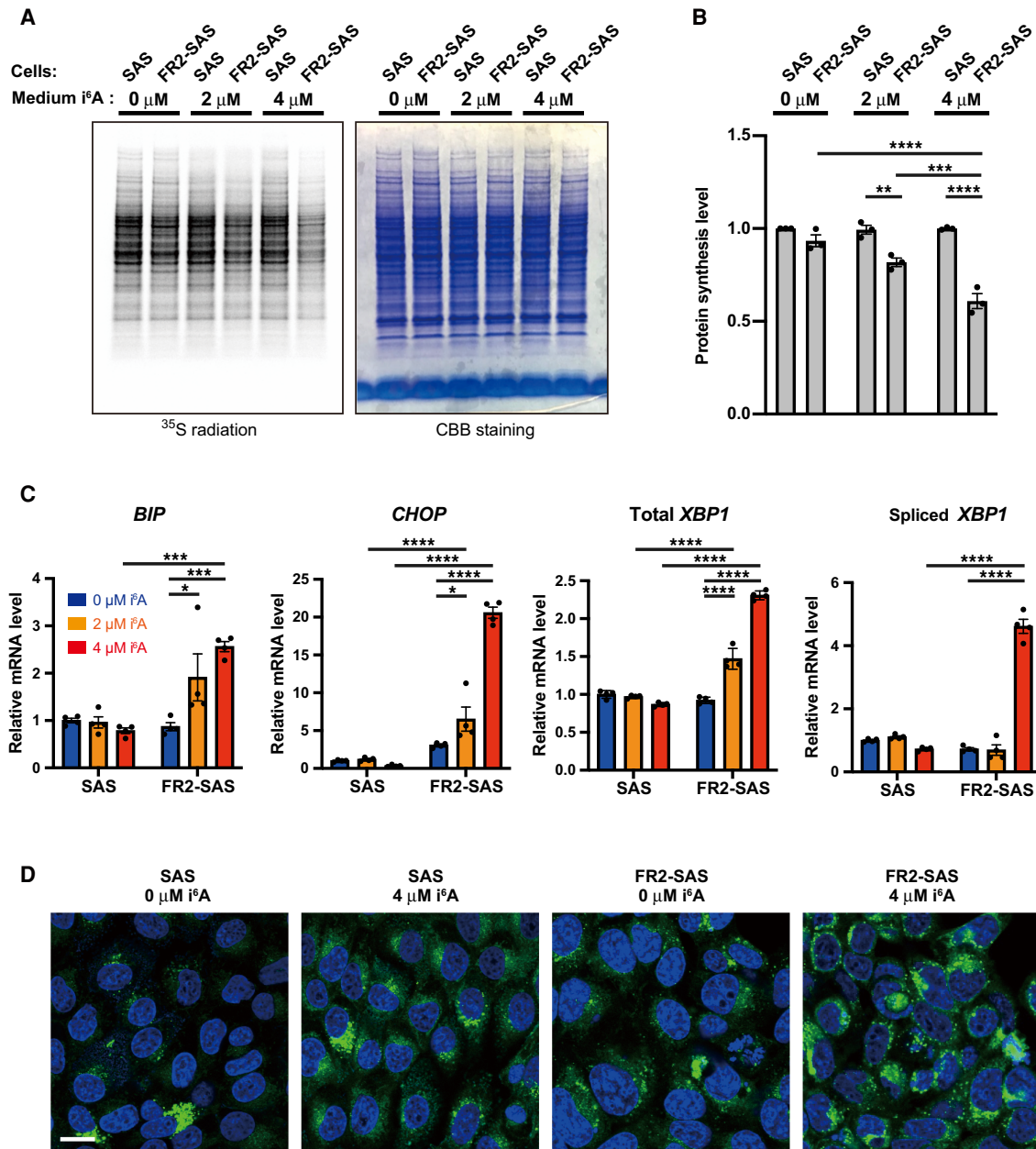


**FIGURE 7.**  $i^6A$ -induced translational decrease and protein aggregation in FR2-SAS cells. (A) Nascent cellular protein synthesis observed by  $^{35}S$ -methionine pulse-labeling. Radiation images of the electrophoresed gel is shown on the *left*, and Coomassie brilliant blue (CBB)-staining of the same gel on the *right* as a loading control.  $n=3$  independent experiments were performed, and representative images are shown. (B) Quantification of the nascent protein signal lanes in A. The relative signal intensities of the lanes versus SAS 0  $\mu M$   $i^6A$  lane were quantified. Mean  $\pm$  SEM from  $n=3$  independent experiments. (C) Quantification of endoplasmic reticulum (ER) stress marker mRNAs by RT-qPCR. Mean  $\pm$  SEM from  $n=4$  biological replicates. RNA levels were normalized by *GAPDH* mRNA levels. (D) Detection of protein aggregation in SAS and FR2-SAS cells. After 24 h of 0 or 4  $\mu M$   $i^6A$  treatment, the cells were fixed and subjected to ProteoStat assay and confocal microscopy. Protein aggregates are shown in green, and Hoechst stained nuclei are shown in blue. Scale bar, 20  $\mu m$ . (\*\*\*\*)  $P < 0.0001$ , (\*\*\*)  $P < 0.001$ , (\*\*)  $P < 0.01$ , (\*)  $P < 0.05$  by two-way ANOVA followed by Tukey's multiple comparison test.

into 18S and 28S rRNAs.  $i^6A$  incorporation occurred in a Pol I-transcription coupled manner and even in cells lacking TRIT1, the cell's sole post-transcriptional  $i^6A$  modifying enzyme. Our data strongly suggest that  $i^6A$  incorporation into rRNAs occurs at the level of transcription, implying

that extracellular  $i^6A$  is imported into cells and phosphorylated to produce  $i^6ATP$ , which is then used for transcription. Considering that 5-FU addition to the medium is known to induce 5-FUTP production and 5-FUrd incorporation into cellular RNA (Kufe and Major 1981; Longley

et al. 2003), we propose that intracellular conversion of *i*<sup>6</sup>A into *i*<sup>6</sup>ATP is the most reasonable hypothesis to explain our results. To investigate this hypothesis, chemical synthesis of authentic *i*<sup>6</sup>ATP and development of a detection method for *i*<sup>6</sup>ATP will be required.

A limitation to our study is that we could not establish causation of *i*<sup>6</sup>A incorporation into RNA and cell death by experiments such as the use of CX-5461 to inhibit Pol I, which would test if *i*<sup>6</sup>A-mediated cell death could be suppressed through a Pol I-mediated mechanism. CX-5461 has itself proven to be cytotoxic, as demonstrated by its use in a phase I clinical trial against hematologic cancers (Khot et al. 2019; Harold et al. 2021). It should be noted that even without *i*<sup>6</sup>A addition, FR2-SAS cells showed more protein aggregation than SAS cells (Fig. 7D, 0  $\mu$ M *i*<sup>6</sup>A SAS and FR2-SAS cells). In addition, the *CHOP* mRNA level was higher in FR2-SAS cells than in SAS cells even without *i*<sup>6</sup>A addition (Fig. 7C, *CHOP* mRNA, blue bars). Thus, FR2-SAS cells might inherently show slightly compromised protein quality, and upon *i*<sup>6</sup>A incorporation into rRNAs, compromised protein quality may further deteriorate and cause ER stress, the excess of which can cause cell death (Hetz et al. 2011). Also, although the majority of *i*<sup>6</sup>A incorporation into RNA depended on Pol I (Fig. 6), it is possible that *i*<sup>6</sup>A also incorporates based on Pol II-mediated mRNA transcription. Such potential *i*<sup>6</sup>A incorporation into mRNA coding sequences might also interfere with mRNA-tRNA interaction in the ribosomes, causing decreased translational speed and decreased translational fidelity.

Generally, artificial analogs of DNA and RNA nucleosides and nucleobases (1) inhibit the function of nucleoside biosynthetic enzymes and/or (2) are used for nucleotide polymerization by DNA/RNA polymerase (Longley et al. 2003; Eyer et al. 2018). 5-FU meets both criteria. Our study strongly suggests that *i*<sup>6</sup>A fits in the latter case and is used in transcription mediated by Pol I. We do not currently know if *i*<sup>6</sup>A inhibits RNA modification enzymes, but our RNA LC-MS experiments, whereby we simultaneously monitored more than 50 modified nucleosides in total RNA, failed to detect observable differences in modification levels of other modified nucleosides, including other *N*<sup>6</sup>-modified adenosines such as *t*<sup>6</sup>A, *ms*<sup>2</sup>*i*<sup>6</sup>A, and *m*<sup>6</sup><sub>2</sub>A (Fig. 4B,C,E).

Extracellular 5-FU has been shown to be imported into cells, converted to 5-FdUTP, and used for DNA synthesis (Longley et al. 2003). We wondered if *i*<sup>6</sup>A can also be converted to deoxy-*i*<sup>6</sup>ATP and used for DNA synthesis. Although our LC-MS cannot detect deoxy-*i*<sup>6</sup>ATP, it can be used to detect the mass equivalent of dephosphorylated deoxy-*i*<sup>6</sup>A. Upon incubation of cells in a medium containing *i*<sup>6</sup>A, we detected a small amount of the mass equivalent to deoxy-*i*<sup>6</sup>A ( $MH^+$   $m/z = 320$ ) from nuclease-digested cellular genomic DNA (Supplemental Fig. 4A). Moreover, the detection occurred in an *i*<sup>6</sup>A concentration-dependent

manner and an *i*<sup>6</sup>A addition time-dependent manner (Supplemental Fig. 4B). The detected peak equivalent to the mass of deoxy-*i*<sup>6</sup>A ( $MH^+$   $m/z = 320$ ) showed a LC retention time 0.4 min after *i*<sup>6</sup>A (Supplemental Fig. 4A). This delay may be due to increased hydrophobicity of deoxy-*i*<sup>6</sup>A compared to *i*<sup>6</sup>A, owing to the lack of the 2' hydroxyl group of ribose, thus making a stronger interaction of deoxy-*i*<sup>6</sup>A with the hydrophobic column in the LC system. In addition, a collision-induced dissociation analysis of this peak detected the mass equivalent to the *N*<sup>6</sup>-isopentenyladenine base ( $MH^+$   $m/z = 204$ ) (Supplemental Fig. 4A). Thus, our preliminary results are in accordance with the presumed conversion of medium-derived *i*<sup>6</sup>A into deoxy-*i*<sup>6</sup>ATP and incorporation into DNA. A conclusive investigation will require chemical synthesis of authentic deoxy-*i*<sup>6</sup>A and deoxy-*i*<sup>6</sup>ATP.

In addition to aberrant translation-mediated effects, considering that the mass equivalent to deoxy-*i*<sup>6</sup>A was detected from the genomic DNA (Supplemental Fig. 4A,B), we should not exclude the possibility of bulky deoxy-*i*<sup>6</sup>A within genomic DNA sterically blocking specific proteins that function on DNA. Moreover, since incorporation of *i*<sup>6</sup>A into rRNAs implies the putative presence of *i*<sup>6</sup>ATP in cells, we cannot exclude the possibility of *i*<sup>6</sup>ATP blocking various enzymatic processes that use ATP, such as phosphorylation, thiolation, and ADP-ribosylation. Therefore, a comprehensive analysis of the cytotoxic mechanisms of *i*<sup>6</sup>A is needed. Such studies may be initiated by performing transcriptome and/or proteome analyses of SAS and FR2-SAS cells that are either treated or not treated with *i*<sup>6</sup>A.

In summary, we searched for means to cause cell death of 5-FU-resistant oral squamous cell carcinoma cell line FR2-SAS and found that *i*<sup>6</sup>A can induce cell death of FR2-SAS cells. *i*<sup>6</sup>A was more effective in inducing cell death in 5-FU-resistant FR2-SAS cells than 5-FU-sensitive parental SAS cells. We also revealed that *i*<sup>6</sup>A addition to the medium induced incorporation of *i*<sup>6</sup>A into cellular 18S and 28S ribosomal RNAs in a Pol I-coupled manner, providing insights into the molecular fate of extracellularly added *i*<sup>6</sup>A in the context of cellular nucleic acid anabolism.

## MATERIALS AND METHODS

### Cell culture

Oral squamous cell carcinoma cell line SAS was acquired from the Cell Resource Center for Biomedical Research in Tohoku University. FR2-SAS cells (originally named SAS/FR2 cells in Nagata et al. 2011) were previously generated from SAS cells (Nagata et al. 2011), and 5-FU-resistance was maintained by culturing the cells in a medium containing 10  $\mu$ M 5-FU. SAS and FR2-SAS cells were grown in Dulbecco's modified Eagle's medium supplemented with 10% fetal bovine serum, in a humidified, 37°C atmosphere with 5% CO<sub>2</sub>. 5-FU (Wako), *i*<sup>6</sup>A (Cayman Chemical Company), CX-5461 (Millipore) or dimethyl sulfoxide (DMSO) vehicle (Nacalai Tesque) were used in experiments.

## Cell number quantification

Both nonadherent cells and adherent cells were collected, mixed and stained with trypan blue (Fujifilm Wako), and alive and dead cells were distinguished and counted using a cell counting device (Olympus). Cells cultured in 96-well plates were quantified using Cell Counting Kit-8 (DOJINBO) and a 96-well plate reader (TECAN).

## Construction of *TRIT1* mutant cells and control cells

Human *TRIT1* mutant cells and control cells were generated using the CRISPR/Cas9 system essentially as described previously (Shalem et al. 2014). Briefly, sense and antisense oligonucleotides encoding a single guide RNA (sgRNA) against *TRIT1* gene or a control sgRNA (not targeting human genome) (Supplemental Table 1; Shalem et al. 2014) were cloned into the BsmBI sites of lentiCRISPR v2 Blast plasmid (Addgene #83480). Lentiviruses were generated in HEK293FT cells by transfecting the sgRNA sequence-containing lentiCRISPR v2 Blast plasmid, psPAX2 plasmid (Addgene #12260) and pMD2.G plasmid (Addgene #12259) with Lipofectamine 3000 (Invitrogen). Fresh HEK293FT cells were transduced with the generated viruses, followed by blasticidin selection of the transduced cells. Subsequently, single clones were acquired by diluting the cells in 96-well plates followed by expansion of the clones. The target region of the genome in each clone was PCR-amplified and sequenced with conventional Sanger sequencing, using the primers listed in Supplemental Table 1.

## RNA extraction

Cells were rinsed with phosphate-buffered saline (PBS) at least three times, and total cellular RNA was prepared using TRI Reagent (MRC), according to the manufacturer's protocol.

## tRNA and rRNA fractionation

Total tRNA fraction was collected from total RNA by electrophoresis of total RNA in denaturing 7 M urea/tris-borate-EDTA (TBE) buffer/10% polyacrylamide gel electrophoresis, staining using SYBR Gold (Invitrogen), gel excision of the tRNA band, and elution of tRNA using 60°C water. 18S and 28S rRNAs were collected by agarose gel electrophoresis of formamide-denatured total RNA, gel excision of rRNA band, and RNA extraction using ZymoClean Gel RNA Recovery Kit (Zymo Research).

## Quantitative reverse-transcription real-time PCR (RT-qPCR)

RT-qPCR was performed as previously described (Takesue et al. 2019). The primer sequences are listed in Supplemental Table 1. For RT-qPCR to detect spliced *XBP1* mRNA, pre-18S rRNA, and pre-28S rRNA, we used previously reported qPCR primers (Chujo et al. 2017; Yoon et al. 2019).

## Genomic DNA extraction

After incubating cells in medium containing 0, 1, or 2  $\mu\text{M}$   $i^6\text{A}$  for 24 or 48 h, cells were rinsed with PBS three times, trypsinized, and collected. The cell pellets were lysed in 1 ml of Proteinase K buffer (20 mM Tris-HCl [pH 8.0], 5 mM EDTA, 400 mM NaCl, 0.3% sodium dodecyl sulfate) and sonicated for a total of 24 sec using Sonifier 250 (Branson) at power 4. Then, 10  $\mu\text{L}$  of Proteinase K (NEB) was added to the solution, and the samples were incubated at 55°C for 1 h for protein digestion, followed by Proteinase K inactivation using phenol-chloroform-isoamylalcohol (Invitrogen). Nucleic acids were collected by isopropanol precipitation, cleaned by 75% ethanol washing, and eluted into 10 mM Tris-HCl (pH 8.0)/1 mM EDTA (pH 8.0). RNA in the solution was digested using RNaseA (Qiagen), and RNaseA was inactivated using phenol-chloroform-isoamylalcohol (Invitrogen). The remaining DNA was isopropanol-precipitated, 75% ethanol-washed, and dissolved into MilliQ water.

## Nucleoside mass spectrometry

RNA or genomic DNA was digested to nucleosides, which were subjected to liquid chromatography triple quadrupole mass spectrometry (LC-MS) using LCMS-8050 (Shimadzu), as previously described (Hirayama et al. 2020; Nagayoshi et al. 2021). A program to detect 5-fluorouridine (molecular weight: 262.2) was added by setting the Q1  $m/z$  to 263.2 Da and Q3  $m/z$  to 131.2 Da with the same collision energy as uridine. The LC elution time and mass spectrum were confirmed by using authentic 5-fluorouridine (Sigma). Programs to detect the DNA-digested nucleosides with the molecular weights equivalent to deoxy- $i^6\text{A}$  (Q1  $m/z$  = 320.0 Da, Q3  $m/z$  = 204.0 Da) and deoxycytidine (Q1  $m/z$  = 228.2 Da, Q3  $m/z$  = 112.1 Da) were added with the same collision energy values as  $i^6\text{A}$  and cytidine, respectively. The LC elution time and mass spectrum of deoxycytidine were confirmed by using authentic deoxycytidine prepared by dephosphorylating dNTP (TOYOBO) with bacterial alkaline phosphatase (TAKARA).

## Western blotting

Western blotting was performed essentially as described previously (Takesue et al. 2019). The antibodies and their conditions for use are listed in Supplemental Table 2.

## $^{35}\text{S}$ -methionine labeling of nascent proteins

Pulse-labeling of nascent proteins was performed essentially as previously described (Fukuda et al. 2021), with some modifications. Briefly, cells grown in 6 cm dishes were incubated in the medium containing 0, 2, or 4  $\mu\text{M}$   $i^6\text{A}$  for 24 h, and briefly washed using 37°C DMEM without Met, Cys, and Gln (Gibco). A total of 3 mL of 37°C preincubation medium (DMEM without Met, Cys, and Gln, supplemented with 2% FBS, 2 mM Gln, 0.2 mM Cys, with 0, 2, or 4  $\mu\text{M}$   $i^6\text{A}$ ) was added to the cells, and the cells were incubated in 37°C  $\text{CO}_2$  incubator for 15 min. The medium was then exchanged with 2 mL of incubation medium (2 mL of preincubation medium containing 5.92 MBq of  $^{35}\text{S}$ -labeled methionine and 0, 2, or 4  $\mu\text{M}$   $i^6\text{A}$ ), and the cells were incubated in 37°C  $\text{CO}_2$  incubator for 35 min. Subsequently, the medium was

removed and the cells were washed with PBS and collected using trypsin and DMEM containing 10% FBS. Cells were lysed and protein concentration was measured using the BCA Protein Assay Kit (Pierce). A total of 20 µg of total proteins were run on Tricine PAGE gel (NOVEX). The gel was stained using Coomassie brilliant blue (CBB) staining solution (Bio-Rad), dried on a gel dryer, photographed, and the radiation image was acquired using an imaging plate and imager (Fujifilm).

### ProteoStat staining assay

A ProteoStat Aggresome Detection Kit (Enzo Life Sciences) was used to monitor protein aggregation. A total of  $4.5 \times 10^5$  SAS or FR2-SAS cells were seeded on 35 mm glass-bottom cell culture dishes (IWAKI), cultured for 48 h, and incubated in the medium containing 0 or 4 µM i<sup>6</sup>A for 24 h. Subsequently, the ProteoStat staining assay was performed according to the manufacturer's instructions, followed by image acquisition using FLUOVIEW FV3000 confocal microscope (Olympus).

### SUPPLEMENTAL MATERIAL

Supplemental material is available for this article.

### ACKNOWLEDGMENTS

We thank the members of the Tomizawa laboratory for fruitful discussions, Yuka Tashiro for technical assistance, and Natalie D. DeWitt for critical reading and language editing. We also thank the Kumamoto University Radioisotope Center at which the <sup>35</sup>S-methionine pulse-labeling experiment was performed. This work was supported by Japan Society for the Promotion of Science KAKENHI grants to K.T. and T.C. (18H02865 and 17KT0054 to K.T., and 20H03187 to T.C.), a Japan Science and Technology Agency FOREST grant to T.C. (JPMJFR204Z), and a Japan Agency for Medical Research and Development grant to K.T. (20gm4010003h0002).

Received March 24, 2022; accepted April 7, 2022.

### REFERENCES

- Agris PF, Eruysal ER, Narendran A, Vare VYP, Vangaveti S, Ranganathan SV. 2018. Celebrating wobble decoding: half a century and still much is new. *RNA Biol* **15**: 537–553. doi:10.1080/15476286.2017.1356562
- Arimbasseri AG, Iben J, Wei FY, Rijal K, Tomizawa K, Hafner M, Maraia RJ. 2016. Evolving specificity of tRNA 3-methyl-cytidine-32 (m<sup>3</sup>C32) modification: a subset of tRNAs<sup>Ser</sup> requires N<sup>6</sup>-isopentenylolation of A37. *RNA* **22**: 1400–1410. doi:10.1261/rna.056259.116
- Aubert M, O'Donohue MF, Lebaron S, Gleizes PE. 2018. Pre-ribosomal RNA processing in human cells: from mechanisms to congenital diseases. *Biomolecules* **8**: 123. doi:10.3390/biom8040123
- Audas TE, Jacob MD, Lee S. 2012. Immobilization of proteins in the nucleolus by ribosomal intergenic spacer noncoding RNA. *Mol Cell* **45**: 147–157. doi:10.1016/j.molcel.2011.12.012
- Beigel JH, Tomashek KM, Dodd LE, Mehta AK, Zingman BS, Kalil AC, Hohmann E, Chu HY, Luetkemeyer A, Kline S, et al. 2020. Remdesivir for the treatment of Covid-19—final report. *N Engl J Med* **383**: 1813–1826. doi:10.1056/NEJMoa2007764
- Boccaletto P, Machnicka MA, Purta E, Piatkowski P, Baginski B, Wirecki TK, de Crecy-Lagard V, Ross R, Limbach PA, Kotter A, et al. 2018. MODOMICS: a database of RNA modification pathways. 2017 update. *Nucleic Acids Res* **46**: D303–D307. doi:10.1093/nar/gkx1030
- Braess J, Freund M, Hanauske A, Heil G, Kaufmann C, Kern W, Schussler M, Hiddemann W, Schleyer E. 1998. Oral cytarabine ocfosfate in acute myeloid leukemia and non-Hodgkin's lymphoma—phase I/II studies and pharmacokinetics. *Leukemia* **12**: 1618–1626. doi:10.1038/sj.leu.2401152
- Carter JM, Emmett W, Mozos IR, Kotter A, Helm M, Ule J, Hussain S. 2019. FICC-Seq: a method for enzyme-specified profiling of methyl-5-uridine in cellular RNA. *Nucleic Acids Res* **47**: e113. doi:10.1093/nar/gkx658
- Castiglioni S, Casati S, Ottria R, Ciuffreda P, Maier JA. 2013. N<sup>6</sup>-isopentenyladenosine and its analogue N<sup>6</sup>-benzyladenosine induce cell cycle arrest and apoptosis in bladder carcinoma T24 cells. *Anticancer Agents Med Chem* **13**: 672–678. doi:10.2174/1871520611313040016
- Cech TR. 2000. Structural biology. The ribosome is a ribozyme. *Science* **289**: 878–879. doi:10.1126/science.289.5481.878
- Chujo T, Tomizawa K. 2021. Human transfer RNA modopathies: diseases caused by aberrations in transfer RNA modifications. *FEBS J* **288**: 7096–7122. doi:10.1111/febs.15736
- Chujo T, Yamazaki T, Kawaguchi T, Kurosaka S, Takumi T, Nakagawa S, Hirose T. 2017. Unusual semi-extractability as a hallmark of nuclear body-associated architectural noncoding RNAs. *EMBO J* **36**: 1447–1462. doi:10.15252/embj.201695848
- Ciaglia E, Abate M, Laezza C, Pisanti S, Vitale M, Seneca V, Torelli G, Franceschelli S, Catapano G, Gazzero P, et al. 2017. Antiglioma effects of N<sup>6</sup>-isopentenyladenosine, an endogenous isoprenoid end product, through the downregulation of epidermal growth factor receptor. *Int J Cancer* **140**: 959–972. doi:10.1002/ijc.30505
- Drygin D, Lin A, Bliesath J, Ho CB, O'Brien SE, Proffitt C, Omori M, Haddach M, Schwaebe MK, Siddiqui-Jain A, et al. 2011. Targeting RNA polymerase I with an oral small molecule CX-5461 inhibits ribosomal RNA synthesis and solid tumor growth. *Cancer Res* **71**: 1418–1430. doi:10.1158/0008-5472.CAN-10-1728
- Eyer L, Nencka R, de Clercq E, Seley-Radtke K, Ruzek D. 2018. Nucleoside analogs as a rich source of antiviral agents active against arthropod-borne flaviviruses. *Antivir Chem Chemother* **26**: 2040206618761299. doi:10.1177/2040206618761299
- Fakruddin M, Wei FY, Suzuki T, Asano K, Kaieda T, Omori A, Izumi R, Fujimura A, Kaitsuka T, Miyata K, et al. 2018. Defective mitochondrial tRNA taurine modification activates global proteostress and leads to mitochondrial disease. *Cell Rep* **22**: 482–496. doi:10.1016/j.celrep.2017.12.051
- Frye M, Jaffrey SR, Pan T, Rechavi G, Suzuki T. 2016. RNA modifications: what have we learned and where are we headed? *Nat Rev Genet* **17**: 365–372. doi:10.1038/nrg.2016.47
- Fukuda H, Chujo T, Wei FY, Shi SL, Hirayama M, Kaitsuka T, Yamamoto T, Oshiumi H, Tomizawa K. 2021. Cooperative methylation of human tRNA<sub>3</sub><sup>Lys</sup> at positions A58 and U54 drives the early and late steps of HIV-1 replication. *Nucleic Acids Res* **49**: 11855–11867. doi:10.1093/nar/gkab879
- Harold CM, Buhagiar AF, Cheng Y, Baserga SJ. 2021. Ribosomal RNA transcription regulation in breast cancer. *Genes (Basel)* **12**: 502. doi:10.3390/genes12040502
- Hetz C, Martinon F, Rodriguez D, Glimcher LH. 2011. The unfolded protein response: integrating stress signals through the stress sensor IRE1α. *Physiol Rev* **91**: 1219–1243. doi:10.1152/physrev.00001.2011

- Hirayama M, Wei FY, Chujo T, Oki S, Yakita M, Kobayashi D, Araki N, Takahashi N, Yoshida R, Nakayama H, et al. 2020. FTO demethylates *cyclin D1* mRNA and controls cell-cycle progression. *Cell Rep* **31**: 107464. doi:10.1016/j.celrep.2020.03.028
- Khalique A, Mattijssen S, Haddad AF, Chaudhry S, Maraia RJ. 2020. Targeting mitochondrial and cytosolic substrates of TRIT1 isopen-tenyltransferase: specificity determinants and tRNA-<sup>i6</sup>A37 profiles. *PLoS Genet* **16**: e1008330. doi:10.1371/journal.pgen.1008330
- Khot A, Brajanovski N, Cameron DP, Hein N, Maclachlan KH, Sanij E, Lim J, Soong J, Link E, Blombery P, et al. 2019. First-in-human RNA polymerase I transcription inhibitor CX-5461 in patients with advanced hematologic cancers: results of a phase I dose-escalation study. *Cancer Discov* **9**: 1036–1049. doi:10.1158/2159-8290.CD-18-1455
- Kufe DW, Major PP. 1981. 5-Fluorouracil incorporation into human breast carcinoma RNA correlates with cytotoxicity. *J Biol Chem* **256**: 9802–9805. doi:10.1016/S0021-9258(19)68695-3
- Laezza C, Caruso MG, Gentile T, Notarnicola M, Malfitano AM, Di Matola T, Messa C, Gazzero P, Bifulco M. 2009. N<sup>6</sup>-isopen-tenyladenosine inhibits cell proliferation and induces apoptosis in a human colon cancer cell line DLD1. *Int J Cancer* **124**: 1322–1329. doi:10.1002/ijc.24056
- Lamichhane TN, Blewett NH, Maraia RJ. 2011. Plasticity and diversity of tRNA anticodon determinants of substrate recognition by eukaryotic A37 isopen-tenyltransferases. *RNA* **17**: 1846–1857. doi:10.1261/rna.2628611
- Lamichhane TN, Mattijssen S, Maraia RJ. 2013. Human cells have a limited set of tRNA anticodon loop substrates of the tRNA isopen-tenyltransferase TRIT1 tumor suppressor. *Mol Cell Biol* **33**: 4900–4908. doi:10.1128/MCB.01041-13
- Longley DB, Harkin DP, Johnston PG. 2003. 5-fluorouracil: mechanisms of action and clinical strategies. *Nat Rev Cancer* **3**: 330–338. doi:10.1038/nrc1074
- Lu ZH, Zhang R, Diasio RB. 1992. Purification and characterization of dihydropyrimidine dehydrogenase from human liver. *J Biol Chem* **267**: 17102–17109. doi:10.1016/S0021-9258(18)41899-6
- Mandel LR, Srinivasan PR, Borek E. 1966. Origin of urinary methylated purines. *Nature* **209**: 586–588. doi:10.1038/209586a0
- Nagata M, Nakayama H, Tanaka T, Yoshida R, Yoshitake Y, Fukuma D, Kawahara K, Nakagawa Y, Ota K, Hiraki A, et al. 2011. Overexpression of cIAP2 contributes to 5-FU resistance and a poor prognosis in oral squamous cell carcinoma. *Br J Cancer* **105**: 1322–1330. doi:10.1038/bjc.2011.387
- Nagayoshi Y, Chujo T, Hirata S, Nakatsuka H, Chen CW, Takakura M, Miyauchi K, Ikeuchi Y, Carlyle BC, Kitchen RR, et al. 2021. Loss of Ftsj1 perturbs codon-specific translation in the brain and is associated with X-linked intellectual disability. *Sci Adv* **7**: eabf3072. doi:10.1126/sciadv.abf3072
- Ogawa A, Nagiri C, Shihoya W, Inoue A, Kawakami K, Hiratsuka S, Aoki J, Ito Y, Suzuki T, Suzuki T, et al. 2021. N<sup>6</sup>-methyladenosine (m<sup>6</sup>A) is an endogenous A3 adenosine receptor ligand. *Mol Cell* **81**: 659–674. doi:10.1016/j.molcel.2020.12.038
- Pane F, Oriani G, Kuo KC, Gehrke CW, Salvatore F, Sacchetti L. 1992. Reference intervals for eight modified nucleosides in serum in a healthy population from Italy and the United States. *Clin Chem* **38**: 671–677. doi:10.1093/clinchem/38.5.671
- Salonga D, Danenberg D, Johnson M, Metzger R, Groshen S, Tsao-Wei D, Lenz H, Leichman C, Leichman L, Diasio R, et al. 2000. Colorectal tumors responding to 5-fluorouracil have low gene expression levels of dihydropyrimidine dehydrogenase, thymidylate synthase, and thymidine phosphorylase. *Clin Cancer Res* **6**: 1322–1327.
- Santi DV, McHenry CS, Sommer H. 1974. Mechanism of interaction of thymidylate synthetase with 5-fluorodeoxyuridylate. *Biochemistry* **13**: 471–481. doi:10.1021/bi00700a012
- Scholler E, Marks J, Marchand V, Bruckmann A, Powell CA, Reichold M, Mutti CD, Dettmer K, Feederle R, Huttenmaier S, et al. 2021. Balancing of mitochondrial translation through METTL8-mediated m<sup>3</sup>C modification of mitochondrial tRNAs. *Mol Cell* **81**: 4810–4825.e4812. doi:10.1016/j.molcel.2021.10.018
- Schweizer U, Bohleber S, Fradejas-Villar N. 2017. The modified base isopen-tenyladenosine and its derivatives in tRNA. *RNA Biol* **14**: 1197–1208. doi:10.1080/15476286.2017.1294309
- Shalem S, Sanjana NE, Hartenian E, Shi X, Scott DA, Mikkelsen TS, Heckl D, Ebert BL, Root DE, Doench JG, et al. 2014. Genome-scale CRISPR-Cas9 knockout screening in human cells. *Science* **343**: 84–87. doi:10.1126/science.1247005
- Shi S, Fukuda H, Chujo T, Kouwaki T, Oshiumi H, Tomizawa K, Wei FY. 2021. Export of RNA-derived modified nucleosides by equilibrative nucleoside transporters defines the magnitude of autophagy response and Zika virus replication. *RNA Biol* **18**: 478–495. doi:10.1080/15476286.2021.1960689
- Spenkuch F, Motorin Y, Helm M. 2014. Pseudouridine: still mysterious, but never a fake (uridine)! *RNA Biol* **11**: 1540–1554. doi:10.4161/15476286.2014.992278
- Spinola M, Galvan A, Pignatiello C, Conti B, Pastorino U, Nicander B, Paroni R, Dragani TA. 2005. Identification and functional characterization of the candidate tumor suppressor gene TRIT1 in human lung cancer. *Oncogene* **24**: 5502–5509. doi:10.1038/sj.onc.1208687
- Suzuki T. 2021. The expanding world of tRNA modifications and their disease relevance. *Nat Rev Mol Cell Biol* **22**: 375–392. doi:10.1038/s41580-021-00342-0
- Takenouchi T, Wei FY, Suzuki H, Uehara T, Takahashi T, Okazaki Y, Kosaki K, Tomizawa K. 2019. Noninvasive diagnosis of TRIT1-related mitochondrial disorder by measuring <sup>i6</sup>A37 and ms<sup>2</sup><sup>i6</sup>A37 modifications in tRNAs from blood and urine samples. *Am J Med Genet A* **179**: 1609–1614. doi:10.1002/ajmg.a.61211
- Takesue Y, Wei FY, Fukuda H, Tanoue Y, Yamamoto T, Chujo T, Shinojima N, Yano S, Morioka M, Mukasa A, et al. 2019. Regulation of growth hormone biosynthesis by Cdk5 regulatory subunit associated protein 1-like 1 (CDKAL1) in pituitary adenomas. *Endocr J* **66**: 807–816. doi:10.1507/endocr.EJ18-0536
- Wei FY, Suzuki T, Watanabe S, Kimura S, Kaitsuka T, Fujimura A, Matsui H, Atta M, Michiue H, Fontecave M, et al. 2011. Deficit of tRNA<sup>Lys</sup> modification by Cdkal1 causes the development of type 2 diabetes in mice. *J Clin Invest* **121**: 3598–3608. doi:10.1172/JCI58056
- Yamamoto T, Fujimura A, Wei FY, Shinojima N, Kuroda JI, Mukasa A, Tomizawa K. 2019. 2-Methylthio conversion of N<sup>6</sup>-isopen-tenyladenosine in mitochondrial tRNAs by CDK5RAP1 promotes the maintenance of glioma-initiating cells. *iScience* **21**: 42–56. doi:10.1016/j.isci.2019.10.012
- Yoon SB, Park YH, Choi SA, Yang HJ, Jeong PS, Cha JJ, Lee S, Lee SH, Lee JH, Sim BW, et al. 2019. Real-time PCR quantification of spliced X-box binding protein 1 (XBP1) using a universal primer method. *PLoS One* **14**: e0219978. doi:10.1371/journal.pone.0219978
- Zhou M, Long T, Fang ZP, Zhou XL, Liu RJ, Wang ED. 2015. Identification of determinants for tRNA substrate recognition by *Escherichia coli* C/U34 2'-O-methyltransferase. *RNA Biol* **12**: 900–911. doi:10.1080/15476286.2015.1050576

**MEET THE FIRST AUTHOR**

Maya Yakita

**Meet the First Author(s)** is a new editorial feature within *RNA*, in which the first author(s) of research-based papers in each issue have the opportunity to introduce themselves and their work to readers of *RNA* and the *RNA* research community. Maya Yakita is the first author of this paper, "Extracellular *N*<sup>6</sup>-isopentenyladenosine (*i*<sup>6</sup>A) addition induces cotranscriptional *i*<sup>6</sup>A incorporation into ribosomal RNAs." Maya is a dentist and a graduate student in the Department of Molecular Physiology in Kumamoto University, Japan.

**What are the major results described in your paper and how do they impact this branch of the field?**

*N*<sup>6</sup>-isopentenyladenosine (*i*<sup>6</sup>A) is an RNA modification that is post-transcriptionally added to a tRNA anticodon loop by a specific tRNA modification enzyme. Using a human oral squamous cell carcinoma (OSCC) cell line, we found that addition of *i*<sup>6</sup>A monomer into the cell culture medium causes the RNA polymerase I to cotranscriptionally incorporate *i*<sup>6</sup>A into ribosomal RNA, accompanied by protein aggregation. We were able to reveal an unexpected molecular fate of extracellularly added modified RNA nucleoside monomer. In addition, we found that *i*<sup>6</sup>A is cytotoxic especially to an OSCC line resistant to the chemotherapeutic drug 5-fluorouracil (5-FU) in a more prominent manner than to its parental 5-FU-sensitive OSCC line.

**What led you to study RNA or this aspect of RNA science?**

I am a dentist. I face patients with oral cancers, as well as cancers that have become resistant to chemotherapy. Some chemotherapeutic drugs such as 5-FU are nucleobase/nucleoside analogs, making me interested in RNA modifications and in entering graduate school to study RNA modifications.

**During the course of these experiments, were there any surprising results or particular difficulties that altered your thinking and subsequent focus?**

*i*<sup>6</sup>A monomer has been known to be cytotoxic, but no one knew its molecular function. After incubating the cells in culture medium containing *i*<sup>6</sup>A, I extracted cellular RNA and checked the RNA modification, just as a control. Then, we were totally surprised and puzzled to detect a lot of *i*<sup>6</sup>A incorporated into total RNA. We could not believe it, so we fractionated total RNA to tRNA and rRNA, and we were further surprised to see that *i*<sup>6</sup>A was incorporated mostly into rRNAs, although endogenous *i*<sup>6</sup>A is a tRNA modification.

**What are some of the landmark moments that provoked your interest in science or your development as a scientist?**

As a graduate student, through studying and struggling with my mentors, I gained confidence on which way to proceed and started to make findings. The more I proceeded, the more I wanted to deepen understanding of my RNA molecules.

**If you were able to give one piece of advice to your younger self, what would that be?**

To find and reach the truth, there is no short cut, but also no waste. If you are having a hard time, it means that you are sincerely doing science, so do not give up, but keep going. At the same time, it is also important to discuss often with the people around you to get good advice.



# RNA

A PUBLICATION OF THE RNA SOCIETY

## Extracellular $N^6$ -isopentenyladenosine ( $i^6A$ ) addition induces cotranscriptional $i^6A$ incorporation into ribosomal RNAs

Maya Yakita, Takeshi Chujo, Fan-Yan Wei, et al.

RNA 2022 28: 1013-1027 originally published online April 12, 2022  
Access the most recent version at doi:[10.1261/rna.079176.122](https://doi.org/10.1261/rna.079176.122)

---

**Supplemental Material**

<http://rnajournal.cshlp.org/content/suppl/2022/04/12/rna.079176.122.DC1>

**References**

This article cites 49 articles, 12 of which can be accessed free at:  
<http://rnajournal.cshlp.org/content/28/7/1013.full.html#ref-list-1>

**Creative Commons License**

This article is distributed exclusively by the RNA Society for the first 12 months after the full-issue publication date (see <http://rnajournal.cshlp.org/site/misc/terms.xhtml>). After 12 months, it is available under a Creative Commons License (Attribution-NonCommercial 4.0 International), as described at <http://creativecommons.org/licenses/by-nc/4.0/>.

**Email Alerting Service**

Receive free email alerts when new articles cite this article - sign up in the box at the top right corner of the article or [click here](#).

---

To subscribe to *RNA* go to:  
<http://rnajournal.cshlp.org/subscriptions>